Ka-Band Radiometric Signatures of Vehicles and Land Surfaces

차량과 지표면의 Ka-대역 레디오미터 신호

Bierng-Chearl Ahn*, Seung-Mo Park**, and Tae-Wook Lim***

안병철*, 박승모**, 임태욱***

Abstract

There have been active research efforts in the development of a dual-use millimeter-wave radiometer as an aircraft landing aid in low visibility conditions. In this paper, we constructed a radiometer operating at the Ka-band where it is relatively easy to build RF components. The radiometer is used to collect radiometric signatures of some vehicles and land surfaces. Measured signatures suggest that vehicles with metallic surfaces yield signatures markedly different from nearby land surfaces so that they can easily be detected by a simple radiometer.

요 약

밀리미터파 대역의 레디오미터를 민군겸용 항공기의 시계 불량시 착륙보조장치로 활용하기 위한 연구가 최근에 활발히 진행되고 있다. 본 논문에서는 이런 관점에서 부품 구현이 비교적 용이한 Ka-대역에서 동작하는 레디오미터를 구성하고 차량과 지형물의 레디오미터 신호를 수집하고 이를 분석하였다. 측정된 신호로부터 마이크로파와 밀리미터파 대역에서 복사율이 낮은 금속차량은 주변 지형물과 확실히 구분되는 신호를 제공함으로써 레디오미터를 사용하여 쉽게 검출될 수 있음을 알 수 있었다.

I. INTRODUCTION

The radiometer technology is a rather mature art finding many diverse and unique applications, among which are atmospheric moisture and temperature profiling, sea surface temperature mapping, subsurface temperature sensing of living tissues[1],[2]. More recently there have been active research efforts in the development of the millimeter-wave radiometer system as an alternative tool for seeing through rain, fog and dust[3]-[7]. The first application of this so-called radio camera is likely to be as landing aids for aircrafts in low visibility conditions.

The modeling of land scenes is an essential part in the development of a passive millimeter-wave imaging system. Numerous investigators have studied the radiometric signature

*충북대학교 전기전자공학부(School of Electrical and Electronic Eng., Chungbuk Univ.)
**(주) 감마 누 웨이브(Gamma Nu Wave, Inc.)
***국방과학연구소(Agency for Defence Development)
· 논문번호 : 98-1-2
· 접수일자 : 1998년 8월 12일

simulation for use in the detection of ground targets[8]-[11]. Hauss, Agravante and Chaiken[11] describe the ARMSS code developed for use in the comprehensive end-to-end scene simulation.

In this paper, we constructed a simple Ka -band radiometer and collected radiometric signatures of some vehicles and land surfaces in view of the ultimate application in the vehicle detection and radio passive imaging. The implementation of a total power radiometric system at the Ka-band is described in some detail followed by discussions on the measurement and properties of radiometric signatures.

Ⅱ. IMPLEMENTATION OF A KA-BAND RADIOMETRIC SYSTEM

Fig. 1 shows a block diagram of a Ka-band heterodyne-type total power radiometer. The thermal radiation in the frequency band of 34.5~35.5 GHz is selected by the IF filter in the receiver chain. The double sideband noise figure of 3.5 dB is combined with the 2.5 dB noise figure of the IF preamplifier yielding an overall system noise figure of 6.0 dB. The receiver noise temperature T_R is now given by

$$T_R = (NF_R - 1)T_0 = 900 \text{ K} \qquad (1)$$

where 300 K is used for the physical temperature T_0 of the receiver.

The equivalent temperature T_A of the thermal radiation received by the antenna ranges from 0 K(objects with zero emissivity) to T_o (=300 K ; objects with unity emissivity). Thus the system noise temperature is given by

$$T_s = T_A + T_R = 900 \text{ to } 1200 \text{ K} \qquad (2)$$

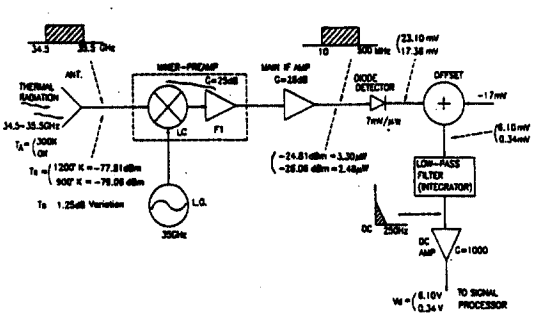

그림 1. Ka-대역 레디오미터의 블록도

Fig. 1. A diagram of a Ka-band radiometer.

The system noise temperature can be represented by the equivalent noise input power

$$P_{in} = KTsB = -79.06 \text{ dBm to } -77.81 \text{ dBm} \qquad (3)$$

The heart of the radiometer technology is to reduce the receiver noise temperature T_R as much as possible so that variations in the received noise temperature T_A introduce as large fractional differences in T_S as possible. Once the range of variations in the received signal power is determined, the next crucial step is to accurately and stably measure an infinitesimal variation in the received power.

After a combined amplification of 53 dB, the signal power at the output of the main IF amplifier

$$P_{out} = G_R P_{in} = -26.06 \text{ dBm to } -24.81 \text{ dBm} \qquad (4)$$

The power level given by (4) is in the middle of the square-law region of typical diode detectors. The sensitivity of the detector is 7 mV/μ W so that the voltage output at the detector is given by

$$V_{D,out} = 17.34 \text{ mV to } 23.10 \text{ mV} \quad (5)$$

To obtain a useful range of variation from (5), we add an offset voltage of −17 mV to $V_{D,out}$ and amplify the resulting voltage by 1, 000 times. The output of the DC amplifier is now given by

$$V_d = 0.34 \text{ to } 6.10 \text{ V} \quad (6)$$

whose level and variation are suitable for the analog-to-digital conversion and the subsequent processing.

The radiometric resolution is limited by noise components in V_d, among which are the long-term drift in the gain of the amplifier chain, change in the offset voltage, and the random noise in the band of DC to 250 Hz. The ratio of the AC component of V_d to the DC component is given by the well-known formula

$$\frac{V_{d.AC}}{V_{d.DC}} = \sqrt{\frac{2B_{LF}}{B_{IF}}} = \sqrt{\frac{2\times 250}{490\times 10^6}} \simeq 0.001 \quad (7)$$

The resolution $\Delta T_{S,min}$ of the radiometric temperatures is now given by

$$\frac{\Delta T_{s,min}}{Ts} = \frac{V_{d.AC}}{V_{d.DC}} = 0.001 \quad (8)$$

so that

$$\Delta T_{s,min} = 0.9 \text{ to } 1.2 \text{ K} \quad (9)$$

The minimum antenna temperature resolvable by the radiometer system is given by (9). From Fig. 1 the change in the received power is 1.25 dB when the equivalent antenna temperature varies from 0 K(cold target) to 300 K(hot target). Thus we can determine the system stability required for observing 1 K difference in the antenna temperature. The result is shown in Table 1.

표 1. $TS = 1$ K를 얻기 위해 요구되는 안정도

Table 1. Stability requirements for $\Delta T_s = 1$ K.

Parameters \ Tolerances	Absolute	Relative (%)
RF Amplifier Gain	± 0.0018 dB	± 0.042
Diode Detector Sensitivity	± 0.0029 mV/μW	± 0.042
Offset Voltage	± 0.0096 mV	± 0.056
DC Amplifier Gain	± 1.6	± 0.16
System Physical Temperature	± 0.5 K	± 0.17

From Table 1 we see that some means of ensuring the system stability are required if accurate radiometric measurements are to be made over a long period. Among stabilizing methods are the noise injection and the Dicke-switching[1]. As a preliminary step toward a practical radiometer instrumentation, we constructed a simple total power radiometer at Ka-band, which was then used to collect radiometric signatures of some vehicles and land surfaces. The data collection was carried out in short period of time so that the system stability was not a major consideration in the measurement.

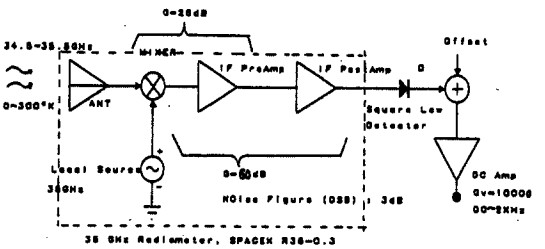

그림 2. 본 연구에서 구성된 레디오미터의 블록도

Fig. 2. A block diagram of the radiometer constructed in this study.

표 2. 레디오미터의 주요 부품

Table 2. Major components of the radiometer.

Components	Specifications	Manufacturer
Antenna	G=33 dB, BW=40° Cassegrain reflector	Spacek
Local Oscillator	f=35 GHz P_o=10 dBm	Spacek
Mixer-IF Preamplifier + IF Main Amplifier	G=60 dB NF=3 dB	Pacific International
Diode Detector	S=1.2mV/μW R_o=15 kΩ	Systron Donner
DC Amplifier	G=10,000 f=DC-2 kHz	Lab. Constructed

Fig. 2 shows the block diagram of the radiometer and Table 2 lists major components of the system. Fig. 3 is a photograph of the instrument set up for measurements.

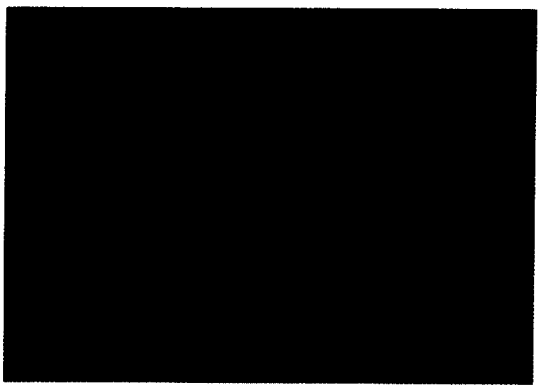

그림 3. 신호파형 측정을 위해 설치된 레디오미터 시스템

Fig. 3. A photograph of the radiometer system set up for measurements.

Ⅲ. MEASUREMENTS AND ANALYSIS OF RADIOMETRIC SIGNATURES

The collection of radiometric signatures is carried out by manually scanning the antenna main beam footprint over the object of interest. Therefore the horizontal axis on signature plots corresponds to the scan time. Fig. 4 shows the scan geometry and Table 3 lists parameters in the scan geometry.

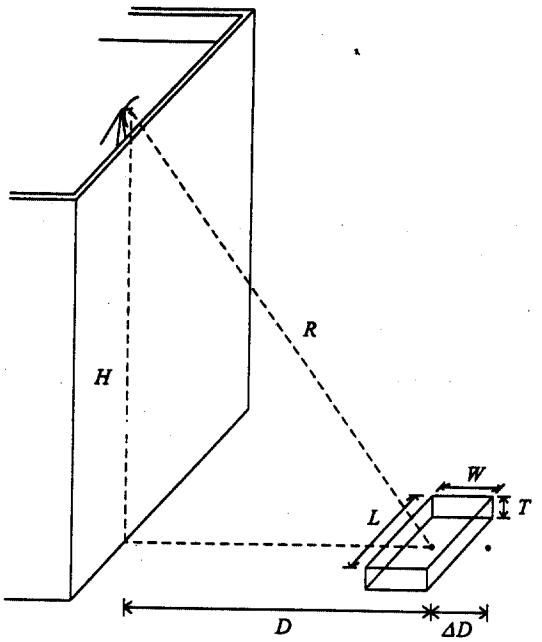

그림 4. 신호파형 수집의 상황도

Fig. 4. The geometry for signature collection.

Measurements are done either on the rooftop or on the ground depending on objects to be scanned.

Fig. 5 to Fig. 11 show measured radiometric signatures. In these figures the offset voltage is set at a convenient level at each measurement. Thus signal levels between plots do not match. Fig. 5 is a sample of radiometric signatures of passenger cars. Three cars are parked on a concrete parking lot and signatures are obtained by scanning the radiometer on the rooftop of a nearby building. In Fig. 5 we first observe that the peak-to-peak noise voltage is about 2 volts, which necessitates an effective

표 3. 신호파형 수집을 위한 스캔 제원

Table 3. Scanning details for signature collection.

Objects	Scan Data	Object Data	Figure No.
Passenger Cars	$H = 13$ m, $D = 14$ m $\Delta D = 0$ m	$L = 4$ m, $W = 1.4$ m $T = 1.2$ m	5
Armored Personal Carrier	$H = 13$ m, $D = 14$ m $\Delta D = -4.0$ to -0.5 m by 0.5 m	$L = 5.5$ m $W = 1.8$ m $T = 1.3$ m	6
Tank	$H = 11$ m, $D = 8.9$ m $\Delta D = -4.0$ to -0.5 m by 0.5 m	$L = 7.3$ m $W = 3.4$ m $T = 2.5$ m	7
Forest	$H = 13$ m, $D = 60$ m	$T = 13$ m	8
Concrete Surface	$H = 13$ m, $D = 13$ m	$T = 0$ m	9
Lake Surface	$H = 1.2$ m, $D = 5 \sim 100$ m	$T = 0$ m	10
Land Scene	$H = 1.2$ m, D 0.5 m	–	11

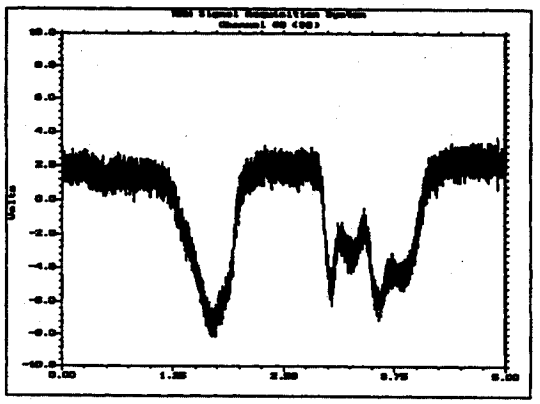

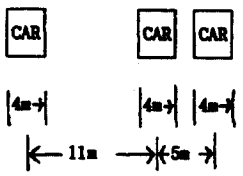

그림 5. 승용차의 레디오미터 신호파형

Fig. 5. The radiometric signature of passenger cars.

low-frequency filter. In this experiment we did not go into details in the instrumentation, because our primary objective is to assess the qualitative nature of radiometric signatures. From Fig. 5 we see that metallic surfaces of automobiles can be easily detected against the concrete background.

Fig. 6 are multiple-scan plots of signatures from an armored personal carrier(APC). Multiple scans are realized by horizontally scanning the antenna with its boresight offset from the center of the vehicle by ΔD. In Fig. 6, labels $A_{-0.5}$, $A_{-1.0}$, etc. denote scanning with $\Delta D = -0.5$ m, -1.0 m, etc., respectively. The swath width of 0.5 meter is achieved by using a telescope mount installed adjacent to the radiometer. In Fig. 6 we see that the contrast between the APC and the ground increases as the antenna footprint covers more of the APC body. This clearly shows the possibility of the passive radio imaging of land vehicles using

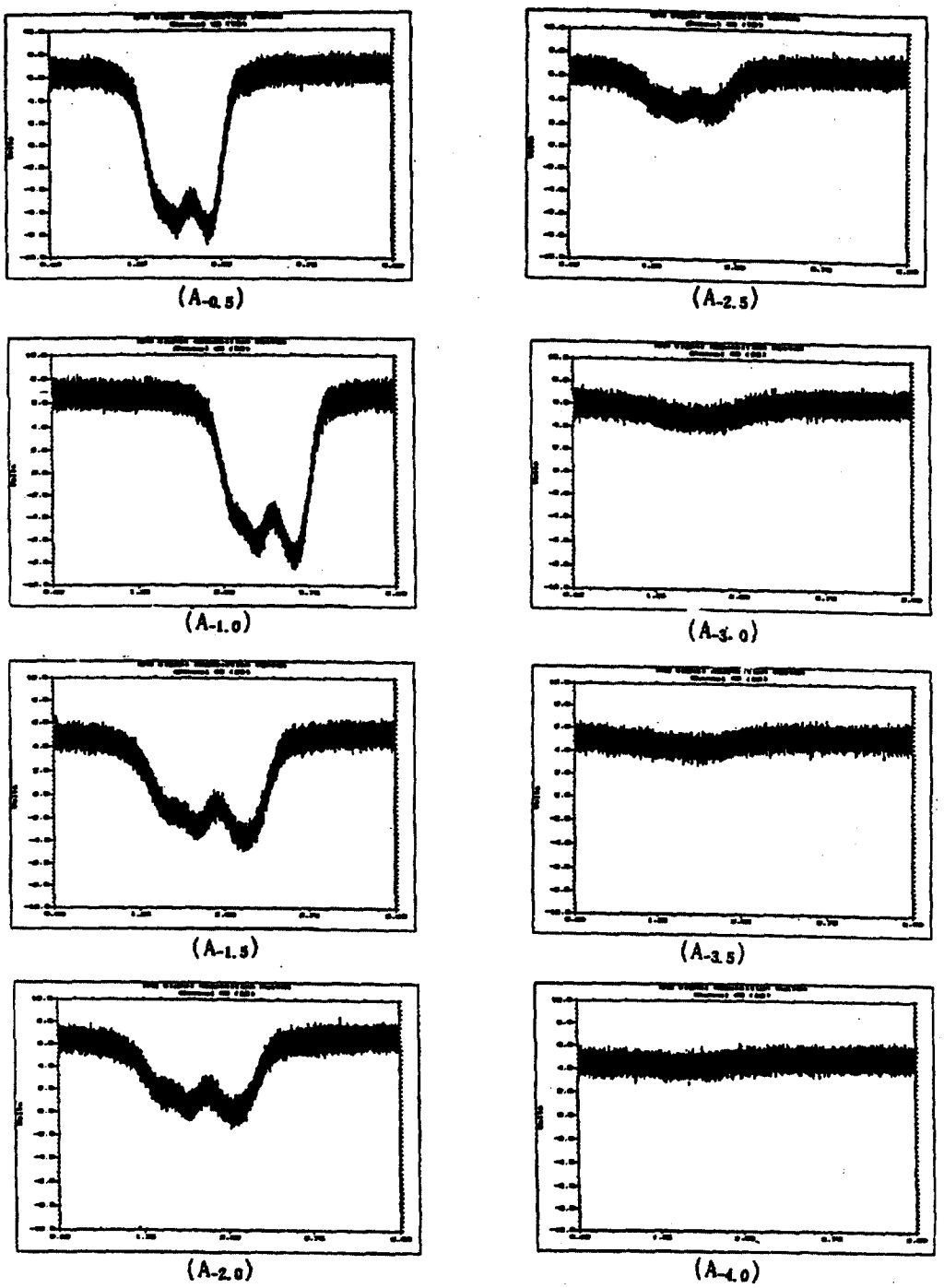

그림 6. 장갑차의 다중스캔 레디오미터 신호파형. 안테나 빔 중심이 표적 중심으로부터 0.5미터 ($A_{0.5}$), 1.0미터($A_{1.0}$),... 등 만큼 떨어졌을 경우.

Fig. 6. Multiple-scan radiometric signatures of an armored personal carrier with the antenna boresight offset from the target center by 0.5 meter($A_{0.5}$), 1.0 meter($A_{1.0}$), ..., etc.

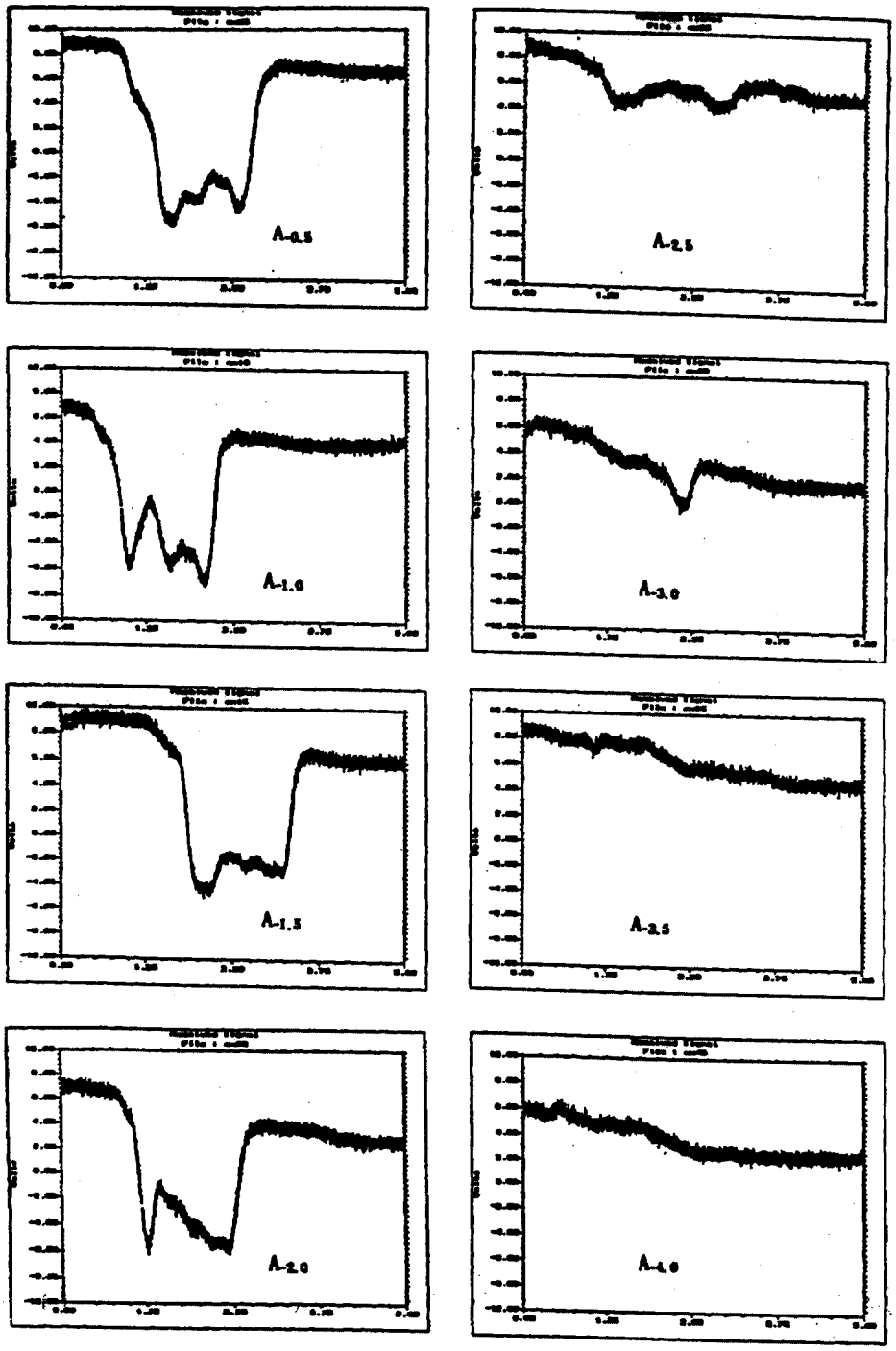

그림 7. 탱크의 다중스캔 레디오미터 신호파형. 안테나 빔 중심이 표적 중심으로부터 0.5미터($A_{-0.5}$), 1.0미터($A_{-1.0}$), ... 등 만큼 떨어졌을 경우

Fig. 7. Multiple-scan radiometric signatures of a tank with the antenna boresight offset from the target center by 0.5 meter($A_{-0.5}$), 1.0 meter($A_{-1.0}$),..., etc.

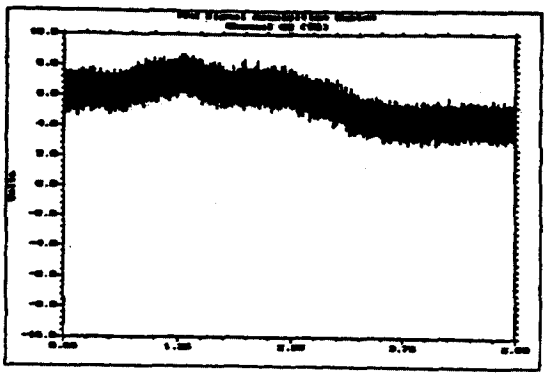

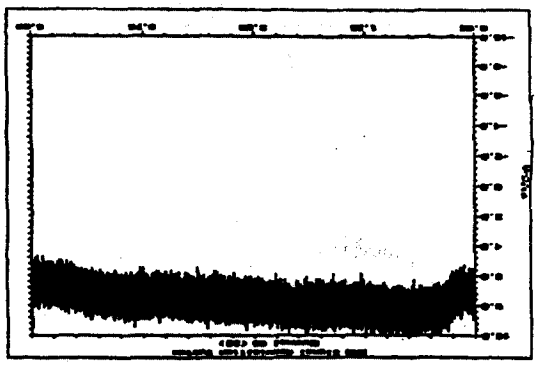

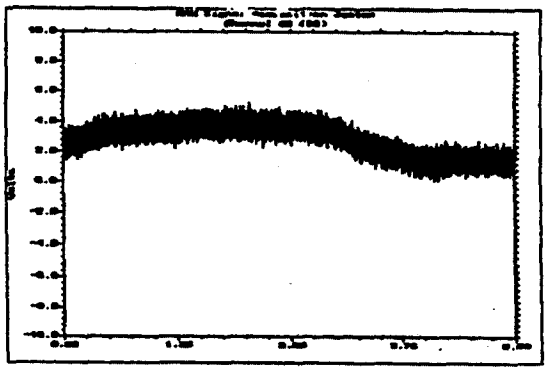

그림 8. 숲의 레디오미터 신호파형의 두 가지 예

Fig. 8. Two samples of the radiometric signature of a forest.

그림 9. 콘크리트 표면의 레디오미터 신호파형의 두 가지 예

Fig. 9. Two samples of the radiometric signature of a concrete surface.

the high-resolution antenna.

Fig. 7 are similar multiple-scan plots of a tank. Here we observe similar signature characteristics. Signatures of the tank are a little more complicated due to the wider, longer and non-flat top surface of the tank.

Fig. 8 and Fig. 9 show radiometric signatures of a foreset and a concrete surface. Here we observe that the radiometric temperature is not sensitive to the look angle, which is typical of electrically rough surfaces. This is in contrast with the signature in Fig. 10, where the radiometer is scanned over a calm water surface of a lake. In the case of a flat surface, the radiometric temperature depends on the look angle.

Fig. 11 shows a sample of radiometric signature of a land scene. It is obtained by contiguously scanning over a lawn(A), a lake surface (B), a hill(C) and the sky(D). As expected the sky is radiometrically cold. It is known that the sky observed vertically yields a radiometric temperature of 30 K at microwave and low millimeter-wave bands.

For a rough calibration of the radiometer, we may use the ground and the sky as reference radiators. An equivalent voltage difference of 44 V is observed when the radiometer points perpendicularly to the 10℃ ground and

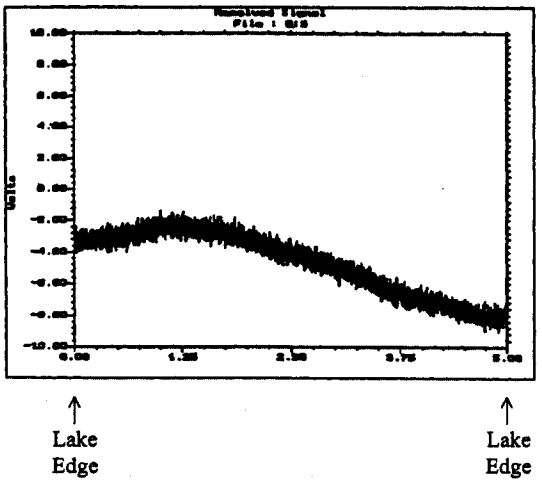

그림 10. 호수면의 레디오미터 신호파형

Fig. 10. The radiometric signature of a lake surface.

to the sky. Assuming a typical emissivity of 0.95 for the ground and the 30 K noise temperature of the sky, we find that the radiometer gives a voltage difference of 184 mV per 1 K change in the observed radiometric temperature.

To determine the radiometric temperature

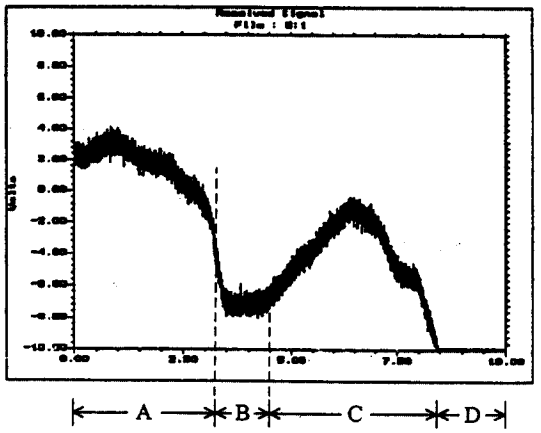

그림 11. 지형의 레디오미터 신호파형

Fig. 11. The radiometric signature of a land scene. A: Lawn, B: Lake, C: Hill, D: Sky.

표 4. 스캔된 물체의 복사온도 계산값

Table 4. Calculated radiometric temperatures of scanned objects.

Objects	Radiometric Temperature (K)	Emissivity
Passenger Car	215	0.76
Armored Personal Carrier	193	0.68
Tank	181	0.64
Land Clutter (Forest, Ground, Concrete)	253~269	0.89~0.95
Water Surface	215	0.76
Sky	30	0.07

from the observed signature, we need to consider the coverage of objects by the antenna footprint. The footprint A of an antenna with a beamwidth of Φ observing an object at an angle of θ from the perpendicular direction is given by

$$A = 0.25\,\pi(R\theta)^2 \sec\theta \tag{10}$$

where R is the slant range. Assuming there are N objects within the antenna footprint, the combined antenna temperature is given by

$$T_A = \frac{1}{A}\sum_{i=1}^{N} A_i T_i \tag{11}$$

where A_i and T_i are the area and radiometric temperature of each object, respectively.

Based on measured signatures and foregoing arguments, radiometric temperatures of scanned objects are calculated and listed in Table 4. Though data in Table 4 are not results of an accurate calibration, they can be used as a useful database in the development of signal processing algorithms for radiometric vehicle

detection systems.

Ⅳ. CONCLUSION

A simple total power radiometer is constructed at Ka-band and used to collect radiometric signatures of vehicles and land surfaces. An analysis is given for a quantitative assessment of stability requirements of the radiometer system. A series of signatures are obtained for such vehicles as passenger cars, armored personal carries, tank, and for land surfaces such as concrete road, lake surface, lawn and forest. Measurements show that metallic vehicles and water surfaces can be easily discerned from surrounding land clutters due to their low radiometric temperatures. A simple calibration of the constructed radiometer system is done by comparing the known radiometric temperatures and measured signatures of the ground and the sky, from which radiometric temperatures and emissivities of scanned objects are calculated.

REFERENCES

[1] N. Skou, *Microwave Radiometer Systems: Design and Analysis*, Norwood, MA: Artech House, 1989.

[2] E. G. Nyfors and P. V. Vainikainen, *Industrial Microwave Sensors*, Norwood, MA: Artech House, 1989, Chapter 7. Radiometer Sensors.

[3] M. A. Burgess and R. D. Hayes, "Synthetic vision - a view in the fog," *IEEE Aerospace and Electronic Systems Magazine*, March 1993.

[4] R. Appleby, S. Price, D. G. Gleed and A. H. Lettington, "Passive millimeter wave imaging: seeing in very poor visibility," *Proc. SPIE Conference on Synthetic Vision for Vehicle Guidance and Control*, Orlando, FL, USA, April 17-18 1995, vol. 2463, pp. 10-19.

[5] M. Shoucri et al., "A passive millimeter wave camera for aircraft landing in low visibility conditions," *IEEE Aerospace and Electronic Systems Magazine*, vol. 10, no. 5, pp. 37-42, May 1995.

[6] R.-C. Chou, J. Loveberg, and C. Martin, "More advances in real-time millimeter-wave imaging radiometers for avionic synthetic vision," *Proc. SPIE Conference on Enhanced and Synthetic Vision*, Orlando, FL, USA, April 21-22 1997, vol. 3088, pp. 2-7.

[7] L. Yujiri *et al.*, "Passive millimeter-wave camera," *Proc. SPIE Conference on Passive Millimeter-Wave Imaging Technology*, Orlando, FL, USA, April 21-22 1997, vol. 3064, pp. 15-22.

[8] D. Ewen, R. Smith, B. Soundstrom, B. Belcher, and K. Trott, "Millimeter-wave analysis of passive signatures (MAPS)," *Proc. SPIE Conference on Passive Millimeter-Wave Imaging Technology*, Orlando, FL, USA, April 21-22 1997, vol. 3064, pp. 2-14.

[9] M. Engel, A. Ben-Shalom, Y. Noiman, and Y. Oreg, "Characterization of passive millimetric wave scenarios: backgrounds and targets at 140 and 220GHz," *Proc. SPIE Conference on Targets and Backgrounds: Characterization and Representation* Ⅲ, Orlando, FL, USA, April 21-23 1997, pp. 151-157.

[10] R. M. Smith, K. D. Trott, B. M. Sundstrom, and D. Ewen, "The passive MM-wave scenario," *Microwave Journal*, vol. 39, no. 3, pp. 22, 24, 26, 28, 30-32,

and 34, March 1996.

[11] B. I. Hauss, H. Agravante, and S. Chaiken, "Advanced radiometric millimeter-wave scene simulation: ARMSS," *Proc. SPIE Conference on Passive Millimeter-Wave Imaging Technology*, Orlando, FL, USA, April 21-22 1997, vol. 3064, pp. 182-193.

안 병 철(安炳哲)

1981년 2월 : 서울대학교 전기공학과 (공학사)

1983년 2월 : 한국과학기술원 전기 및 전자공학과(공학석사)

1992년 12월 : University of Mississippi, Electrical Engineering(공학박사)

1983년 3월~1986년 7월 : LG정밀(주) 주임연구원

1993년 1월~1995년 2월 : 국방과학연구소 선임연구원

1995년 3월~현재 : 충북대학교 전기전자공학부 조교수

관심분야 : RF시스템, 레이더, 안테나, 전자장 모델링

임 태 욱(林泰旭)

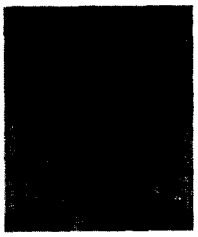

1990년 2월 : 인하대학교 전자공학과 (공학사)

1990년 3월~현재 : 국방과학연구소 선임연구원

관심분야 : RF회로설계, 안테나, RF시스템

박 승 모(朴承模)

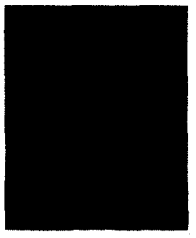

1985년 : 경북대학교 전자공학과 (공학사)

1987년 : 경북대학교 전자공학과 (공학석사)

1987년 2월~1997년 11월 : 국방과학연구소 선임연구원

1997년 12월~현재 : (주)감마 누 웨이브, RF소자개발팀장

관심분야 : RF회로설계, 안테나, 이동통신용 RF분야